ICESAT LIDAR AND GLOBAL DIGITAL ELEVATION MODELS: APPLICATIONS TO DESDYNI

Claudia C. Carabajal[1], *David J. Harding*[2] *and Vijay P. Suchdeo*[1]

[1] Sigma Space Corp. @ NASA Goddard Space Flight Center, Planetary Geodynamics Laboratory, Code 698, Greenbelt, MD 20771, USA.

[2] NASA Goddard Space Flight Center, Planetary Geodynamics Laboratory, Code 698, Greenbelt, MD 20771, USA.

ABSTRACT

Geodetic control is extremely important in the production and quality control of topographic data sets, enabling elevation results to be referenced to an absolute vertical datum. Global topographic data with improved geodetic accuracy achieved using global Ground Control Point (GCP) databases enable more accurate characterization of land topography and its change related to solid Earth processes, natural hazards and climate change. The multiple-beam lidar instrument that will be part of the NASA Deformation, Ecosystem Structure and Dynamics of Ice (DESDynI) mission will provide a comprehensive, global data set that can be used for geodetic control purposes. Here we illustrate that potential using data acquired by NASA's Ice, Cloud and land Elevation Satellite (ICEsat) that has acquired single-beam, globally distributed laser altimeter profiles (± 86°) since February of 2003 [1, 2]. The profiles provide a consistently referenced elevation data set with unprecedented accuracy and quantified measurement errors that can be used to generate GCPs with sub-decimeter vertical accuracy and better than 10 m horizontal accuracy. Like the planned capability for DESDynI, ICESat records a waveform that is the elevation distribution of energy reflected within the laser footprint from vegetation, where present, and the ground where illuminated through gaps in any vegetation cover [3]. The waveform enables assessment of Digital Elevation Models (DEMs) with respect to the highest, centroid, and lowest elevations observed by ICESat and in some cases with respect to the ground identified beneath vegetation cover. Using the ICESat altimetry data we are developing a comprehensive database of consistent, global, geodetic ground control that will enhance the quality of a variety of regional to global DEMs. Here we illustrate the accuracy assessment of the Shuttle Radar Topography Mission (SRTM) DEM produced for Australia, documenting spatially varying elevation biases of several meters in magnitude.

Index Terms— ICESat, global geodetic control, laser altimetry, DEM accuracy, elevation errors, DESDynI

1. INTRODUCTION

Accurate laser altimeter elevation profiles contribute to a number of Solid Earth science and applied objectives. A primary contribution is the independent characterization of systematic and random elevation errors in Digital Elevation Models (DEMs) produced by photogrammetric and Interferometric SAR techniques. This kind of quality assessment enables DEMs to be used quantitatively for purposes for which their accuracy is appropriate. In addition to evaluating DEM accuracy, laser altimeter profiles can be used in the correction of systematic errors in DEMs, improving their utility for detection of elevation change observed by differencing DEMs obtained at different times. NASA's Deformation, Ecosystem Structure and Dynamics of Ice (DESDynI) mission, scheduled for launch later this decade, will provide globally distributed laser altimeter profiles well suited for these purposes. It will simultaneously acquire multiple profiles with 25 m diameter, nearly-contiguous laser footprints along the profiles. Although NASA's Ice, Cloud and land Elevation Satellite (ICESat) has less dense sampling (a single profile with ~50 m footprints spaced 175 m apart), it illustrates the capabilities for accuracy assessment and control of DEMs that will be significantly expanded by DESDynI.

We have previously used ICESat data to evaluate the accuracy of the 90 m resolution, near-global DEM produced by the Shuttle Radar Topography Mission (SRTM) [4, 5, 6] and the more recent global ASTER DEM [7]. The Geoscience Laser Altimeter System (GLAS) aboard ICESat acquired data from 2003 to 2009, during month-long observant periods that were conducted three, and later two, times a year. Figure 1 shows an example assessment of SRTM accuracy using an ICESat profile. The negative-elevation differences reveal that the SRTM DEM is biased high relative to an absolute datum by several meters, on average, across western Australia. In addition, the along-profile variations reveal undulating elevation errors in the SRTM DEM at the 100s of kilometer length scale and ~5 m amplitude. ICESat data documents the spatial structure of these undulations, which can then be removed from the DEM. The comprehensive, near global (± 86°) ICESat

coverage across continents enables correction of long-wavelength DEM errors not previously made possible by other means. Here we present results for along-profile and gridded elevation differences between ICESat geodetic control data and the SRTM DEM for Australia, documenting the spatial pattern and magnitude of elevation errors in that DEM. We do this using each ICESat observation period separately, documenting that the ICESat results are highly reproducible.

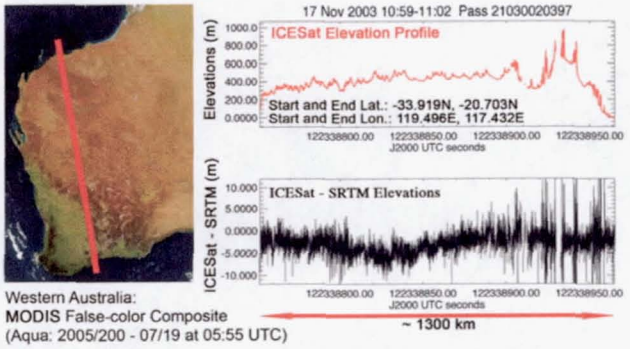

Figure 1. Elevation measurements (top right) along an ICESat profile in western Australia (left, red line on MODIS image) and differences with the SRTM DEM (bottom right) for individual ICESat laser footprints.

2. DEVELOPMENT OF A GLOBAL ICESAT GEODETIC CONTROL DATABASE

Using the ICESat Land/Canopy Elevation data product (GLA14), we are producing a global set of GCPs in a project supported by NASA's Earth Surface and Interior Program. We apply stringent editing criteria in order to produce the highest quality ground control. For this paper, we have used the latest public release of the ICESat 91-day repeat track data (Release 31). Like the DESDynI lidar will do, the GLAS instrument records a waveform, the height distribution of energy reflected from illuminated vegetation and ground surfaces in the laser footprint. In addition to providing the latitude, longitude and derived elevations for each ICESat waveform referenced to the Topex/Posseidon (T/P) ellipsoid, the GLA14 product also includes the SRTM DEM elevation at the footprint location. The publically distributed finished SRTM DEM contains orthometric elevations produced using the EGM96 geoid [8]. On the GLA14 Release 31 product that we are using the SRTM elevations have been converted to ellipsoidal values, but by incorrectly applying the more recent EGM08 geoid. We therefore correct the SRTM ellipsoidal heights in the products using the SRTM reference geoid, EGM96. We then compute the elevation differences between the SRTM radar phase center elevation and four elevations derived from the ICESat waveform: the highest observed surface (waveform start), the waveform centroid (average elevation), the lowest observed surface (waveform end) and, where possible, the ground elevation inferred from the lowest Gaussian fit derived from waveform modeling. We also obtain a land cover classification for each laser footprint from the MERIS Globcover land cover regional product (51 possible classes), derived by an automatic and regionally-tuned classification of a MERIS FR time series [9]. The MERIS product is generated at 300 m resolution using data from the period December 2004 – June 2006.

We apply stringent editing criteria to yield a high quality GCP database. We exclude ICESat data identified as returns from water (MERIS land cover = 210). We also exclude ICESat returns inferred to be from clouds using a threshold 50 m above the SRTM surface at the laser footprint location. The cloud flag in the ICESat products indicating a clear atmosphere proved too severe for editing and was not reliable for periods when the transmit laser energy was low. One of the main criteria for obtaining the most accurate ground control data is selection of waveforms from relatively non-vegetated areas with low relief. We do so by limiting the width of the selected waveforms (signal start to signal end) to 5 m. For these narrow waveforms the elevations for the waveform centroid and the ground lowest Gaussian fit essentially coincide.

We also apply editing based on instrumental parameters. Weak returns are excluded by only using returns with maximum amplitudes greater than 0.15 Volts. Where the return energy exceeds the receiver's dynamic range, the GLAS waveforms become saturated. Saturation broadens, distorts and truncates the received waveforms. Although laboratory calibrations developed as a function of receiver gain and observed received energy exist to correct elevations and receive energies, we only keep non-saturated to minimally saturated data where the saturation index (the number of waveform bins with an amplitude greater than the saturation threshold) is two or less. The accuracy of the ICESat data is degraded with increasing incidence angle between the laser beam vector and the normal to the surface slope, causing waveform broadening. To minimize this error source, we exclude data acquired when the laser beam was pointed off from nadir by more than 1°. Rigorous analysis has shown that for low relief locations the ICESat data meet the accuracy requirements of 6 m horizontal and 10 cm vertical [S. Luthcke, pers. comm.]. Because we use stringent editing criteria we expect that our GCPs are of equivalent accuracy.

Table 1 presents elevation difference between our ICESat GCPs and SRTM, computed as ICESat minus SRTM, for Australia. Results are given for ICESat observation periods acquired with the 2nd (L2) and 3rd (L3) laser transmitters, with their start and end dates and average laser transmit energies indicated (for each laser the transmit energy started high, causing substantial saturation, and then dropped significantly during the course of the mission).

Figure 2 illustrates ICESat minus SRTM difference histograms for ICESat's highest, centroid and lowest elevations using a representative observation period (L3E), showing well-defined normal distributions. Like the other

periods, this period shows an SRTM elevation bias with respect to the ICESat centroid of ~ -2 m.

Laser Period	D	N*	N	M	S	R
L2A	H	1219818	106868	0.66	3.53	2.46
10/4/03-11/19/03	C	8.76%	106868	-1.86	3.68	2.96
E (fJ)**	G		106868	-1.92	3.66	3.00
70.7	L		106868	-3.87	3.53	4.50
L2B	H	891185	274844	0.27	5.72	2.28
2/17/04-3/21/04	C	30.84%	274844	-1.96	5.46	2.98
E (fJ)	G		274844	-1.98	5.48	2.99
45.6	L		274844	-3.96	5.72	4.56
L2C	H	909511	473896	-0.10	8.03	2.37
5/18/04-6/21/04	C	52.10%	473896	-2.11	7.75	3.16
E (fJ)	G		473896	-2.14	7.70	3.19
12.5	L		473896	-3.89	8.03	4.56
L3A	H	1098000	327543	0.32	4.89	2.26
10/3/04-11/8/04	C	29.83%	327543	-1.95	4.71	2.95
E (fJ)	G		327543	-1.96	4.72	2.96
63.7	L		327543	-3.98	4.89	4.56
L3B	H	979204	316537	0.19	3.13	2.23
2/17/05-3/24/05	C	32.33%	316537	-2.01	3.04	2.98
E (fJ)	G		316537	-2.01	3.02	2.98
59.1	L		316537	-4.02	3.13	4.58
L3C	H	948062	387123	0.11	2.74	2.23
5/20/05-6/23/05	C	40.83%	387123	-1.97	2.74	2.96
E (fJ)	G		387123	-1.96	2.73	2.96
45.5	L		387123	-3.94	2.74	4.52
L3D	H	995164	452400	0.00	3.92	2.23
10/21/05-11/24/05	C	45.46%	452400	-2.07	3.71	3.05
E (fJ)	G		452400	-2.06	3.69	3.04
39.4	L		452400	-4.04	3.92	4.63
L3E	H	835701	380954	-0.06	5.03	2.23
2/22/06-3/28/06	C	45.58%	380954	-2.08	4.70	3.05
E (fJ)	G		380954	-2.07	4.67	3.05
34.1	L		380954	-4.05	5.03	4.63
L3F	H	1036357	438987	0.09	5.09	2.25
5/24/06-6/26/06	C	42.36%	438987	-2.00	4.84	3.01
E (fJ)	G		438987	-1.99	4.83	3.00
30.8	L		438987	-4.01	5.09	4.59
L3G	H	969972	455341	0.01	3.58	2.28
10/25/06-11/27/06	C	46.94%	455341	-2.06	3.49	3.07
E (fJ)	G		455341	-2.05	3.47	3.06
27.1	L		455341	-4.04	3.58	4.65
L3H	H	883219	422979	-0.05	5.05	2.26
3/12/07-4/14/07	C	47.89%	422979	-2.09	4.89	3.08
E (fJ)	G		422979	-2.08	4.87	3.08
22.6	L		422979	-4.06	5.05	4.65
L3I	H	967652	488675	-0.15	3.85	2.27
10/2/07-11/5/07	C	50.50%	488675	-2.15	3.69	3.13
E (fJ)	G		488675	-2.13	3.69	3.12
20.5	L		488675	-4.12	3.85	4.72
L3J	H	922899	447482	-0.13	4.16	2.24
2/17/08-3/21/08	C	48.49%	447482	-2.13	3.89	3.09
E (fJ)	G		447482	-2.11	3.87	3.08
17.7	L		447482	-4.11	4.16	4.69
L3K	H	450592	231122	-0.23	7.10	2.38
10/4/08-10/19/08	C	51.29%	231122	-2.20	6.72	3.23
E (fJ)	G		231122	-2.17	6.70	3.22
15.6	L		231122	-4.16	7.10	4.79
L2D	H	554068	374051	-0.44	7.60	2.44
11/25/08-12/17/08	C	67.51%	374051	-2.34	7.34	3.36
E (fJ)	G		374051	-2.38	7.29	3.39
5.4	L		374051	-4.06	7.60	4.73

Table 1. ICESat – SRTM Elevation Difference Statistics

D = Differences (H: Highest; C: Centroid; L: Lowest; G: ground)

N* = Number of returns classified as be from the Earths's surface and the percent retained after editing

N = Number of returns after editing

M =Mean elevation difference; S = standard deviation; R = RMSE

E (fJ)** = Average transmit energy corrected for receiver field of view (FOV) shadowing

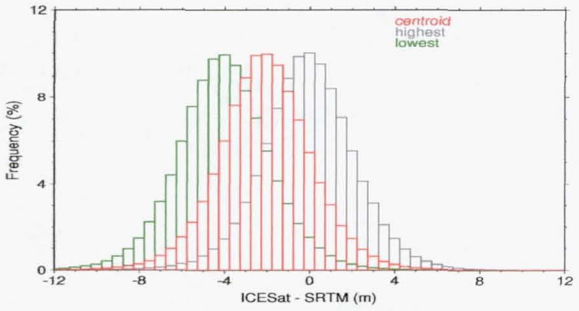

Figure 2. Elevation difference histograms for ICESat highest, centroid and lowest minus SRTM for the L3E laser observation period (See Table 1 for complete statistics).

Examination of the centroid differences for all laser periods (Figure 3) shows very consistent mean elevation difference results, a demonstration of ICESat's highly accurate and reproducible absolute elevations. There is a slightly decreasing trend with laser energy decay, especially for Laser 2 (L2), potentially related to the large number of edited saturated returns during early, high energy periods. This could cause a bias by preferentially removing areas of high surface reflectivity. The origin of this L2 drift and the associated increase in standard deviation requires further investigation.

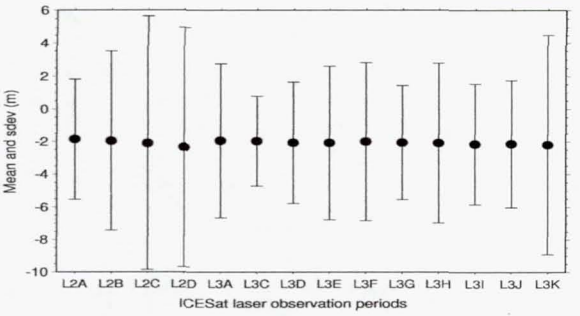

Figure 3. Mean ICESat centroid minus SRTM elevation differences and standard deviations for all ICESat observation periods (See Table 1 for complete statistics).

3. DERIVED CORRECTION SURFACES FOR AUSTRALIA

After selecting the ground control database for each ICESat period, we obtain a representation of the undulations in ICESat centroid minus SRTM differences in two different ways. First, we apply a sliding boxcar filter along every edited ICESat profile at 1° intervals (Figure 4, top). Alternatively, we divide the region in 1° by 1° tiles, and compute the mean differences and their standard deviations for the points within each tile (Figure 4, lower 3 panels). Both the along-profile and gridded representations highlight long wavelength elevation-error undulations in the SRTM DEM of several meters magnitude.

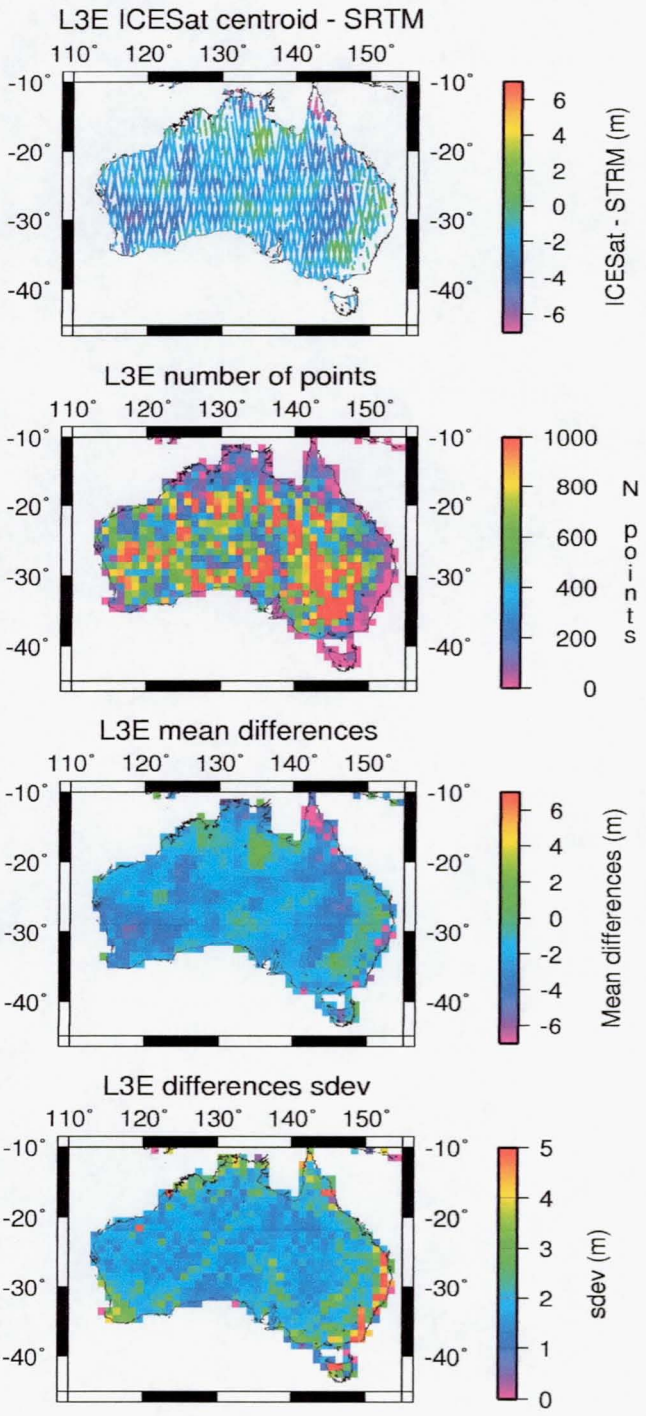

Figure 4. Mean ICESat centroid – SRTM differences for the L3E observation period. Differences computed using a 1° along track sliding box-car filter are shown on the top, and 1° gridded averages and their standard deviations for the indicated number of returns in a cell are shown in the three lower panels. Colors indicate ranges shown by the color bars.

4. CONCLUDING REMARKS AND APPLICATION TO THE DSDYNI MISSION

Profiling spaceflight laser altimeters make important contributions to the solid Earth Science by providing accurate, global, consistently referenced, geodetic elevation data. Expanding upon the Australia work described here, our ICESat GCP dataset is contributing to a global, coordinated and integrated DEM database produced from different sources, embedded into a consistent, high accuracy, and long term stable geodetic reference frame. It will be particularly useful in northern and southern latitudes above and below ±60°, where high-resolution topographic data assets are not available and topographic control is scarce. Methodologies developed to use ICESat data for global geodetic control purposes are a pathfinder for similar use of data to be produced by the lidar component of the DESDynI mission. With substantially improved sampling as compared to ICESat, DESDynI will provide a more comprehensive set of global GCPs from it's multi-beam, higher-resolution elevation profiles.

REFERENCES

[1] Zwally, H.J., R. Schutz, W. Abdalati, J. Abshire, C. Bentley, J. Bufton, D. Harding, T. Herring, B. Minster, J. Spinhirne and R. Thomas, 2002, ICESat's laser measurements of polar ice, atmosphere, ocean, and land, *Journal of Geodynamics*, 34(3-4), 405-445.

[2] Schutz, B. E., H. J. Zwally, C. A. Shuman, D. Hancock, and J. P. DiMarzio (2005), Overview of the ICESat Mission, *Geophys. Res. Lett.*, 32, L21S01, doi:10.1029/2005GL024009.

[3] Harding, D.J., and C.C. Carabajal, 2005, ICESat Waveform Measurements of Within-footprint Topographic Relief and Vegetation Vertical Structure, *Gephys. Res. Lett.*, L21S10, 10.1029/2005GL023471.

[4] Farr, T. G., et al., 2007, The Shuttle Radar Topography Mission, *Rev. Geophys.*, 45, RG2004, doi:10.1029/2005RG000183.

[5] Carabajal, C.C., and D. J. Harding, 2005, ICESat validation of SRTM C-band digital elevation models, *Geophys. Res. Let.*,32, L22S01, doi:10.1029/2005GL023957.

[6] Carabajal, C.C. and D. J. Harding, 2006, SRTM C-band and ICESat Laser Altimetry Elevation Comparisons as a Function of Tree Cover and Relief, *Photogram. Eng. and Rem. Sens.*, 72(3), 287-298.

[7] ASTER GDEM Validation Team: METI/ERSDAC, NASA/LPDAAC, USGS/EROS, 2009, in cooperation with NGA and Other Collaborators, *ASTER Global DEM Validation Summary Report*:https://lpdaac.usgs.gov/lpdaac/products/aster_products_table/routine/global_digital_elevation_model/v1/astgtm.

[8] Slater, J.A., Garvey, G., Johnston, C., Haase, J., Heady, B., Kroenung, G. and Little, J., 2006, The SRTM Data Finishing Process and Products, *Photogrammetric Engineering and Remote Sensing*, 772(3), pp. 237-248.

[9] http://www.esa.int/due/ionia/globcover; Source Data: © ESA / ESA Globcover Project, led by MEDIAS-France/POSTEL).